SAMSO TR-69-145

AD689220

CHEMICAL KINETICS OF COF_2 DECOMPOSITION IN SHOCK WAVES

Prepared by

AVCO GOVERNMENT PRODUCTS GROUP
SPACE SYSTEMS DIVISION
LOWELL INDUSTRIAL PARK
Lowell, Massachusetts 01851

AVSSD-0247-68-RR
Contract F04-701-68-C-0036

15 November 1968

Prepared for

ADVANCED RESEARCH PROJECTS AGENCY
DEPARTMENT OF DEFENSE
AND
SPACE AND MISSILE SYSTEMS ORGANIZATION

Monitored by

SPACE AND MISSILE SYSTEMS ORGANIZATION
DEPUTY FOR REENTRY SYSTEMS
AIR FORCE SYSTEMS COMMAND
Norton Air Force Base, California 92409

DISCLAIMER NOTICE

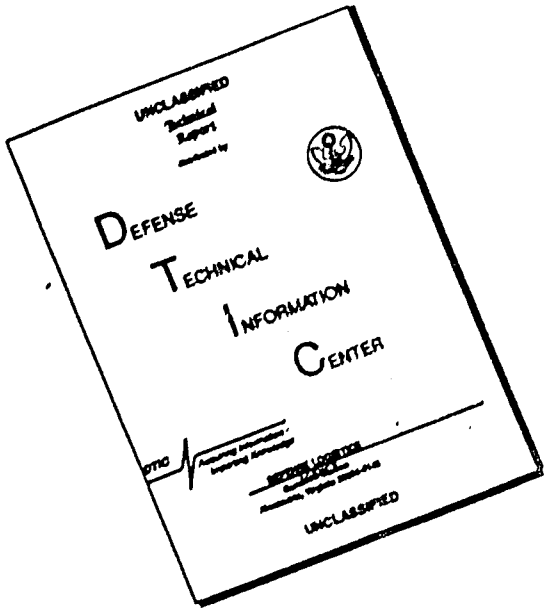

THIS DOCUMENT IS BEST QUALITY AVAILABLE. THE COPY FURNISHED TO DTIC CONTAINED A SIGNIFICANT NUMBER OF PAGES WHICH DO NOT REPRODUCE LEGIBLY.

SAMSO TR-69-145

CHEMICAL KINETICS OF COF_2 DECOMPOSITION IN SHOCK WAVES

Prepared by

AVCO GOVERNMENT PRODUCTS GROUP
SPACE SYSTEMS DIVISION
LOWELL INDUSTRIAL PARK
Lowell, Massachusetts 01851

AVSSD-0247-68-RR
Contract F04-701-68-C-0036

by

A. P. Modica

15 November 1968

Prepared for

ADVANCED RESEARCH PROJECTS AGENCY
DEPARTMENT OF DEFENSE
AND
SPACE AND MISSILE SYSTEMS ORGANIZATION

Monitored by

SPACE AND MISSILE SYSTEMS ORGANIZATION
DEPUTY FOR REENTRY SYSTEMS
AIR FORCE SYSTEMS COMMAND
Norton Air Force Base, California 92409

ABSTRACT

An infrared technique has been used to monitor the thermal decomposition of carbonyl fluoride (COF_2) in argon and nitrogen diluent behind incident and reflected shock waves. Data was taken in the temperature range 2400° to 3600° K at total pressures between 0.2 and 26 atm. Direct sampling of reflected shock mixtures with a time-of-flight mass spectrometer provided knowledge of the decomposition products. The pressure and temperature dependence of the COF_2 dissociation rate constants are discussed in terms of the Rice-Ramsperger-Kassel (RRK) unimolecular theory. Rate constants for the fluorine extraction reactions and CF disproportionation reaction were obtained by curve-fitting the complete COF_2 kinetic histories with computed profiles. A chemical nonequilibrium stream-tube program which includes wall boundary layer effects was used for data analysis.

EDITED BY:
EDITORIAL SERVICES SECTION
J.F. Thompson

CONTENTS

ILLUSTRATIONS

TABLES

FOREWORD

The present study was conducted in the Chemical Physics Research Group of the Avco Corporation Space Systems Division's Aerophysics Laboratory and was supported by the Advanced Research Projects Agency under subcontract from the Avco Everett Research Laboratory through Contract F04-701-68-C-0036, part of Project Defender.

ACKNOWLEDGEMENT

The author expresses thanks to S. J. Sillers for programming the chemical non-equilibrium stream-tube computer problem and to R. R. Brochu for assisting in the collection and reduction of the shock-tube data.

I. INTRODUCTION

At present the chemical rates for fluorocarbon decomposition and oxidation kinetics are needed for input to a number of aerospace engineering problems. Mass spectrometer study on the pyrolysis of Teflon plastic (polytetrafluoroethylene) in atmospheres of air and oxygen[1] shows that carbonyl fluoride (COF_2) is an important low-temperature (800° K) oxidation intermediate and that at higher temperatures carbon dioxide (CO_2) and perfluoromethane (CF_4) dominate the reaction products. Measurements to identify the infrared and visible spectrum of an air-Teflon boundary layer in a hot subsonic arc jet have shown the presence of the CN-violet and red bands and structure in the 2 to 6μ region characteristic of the COF_2, CO and CO_2 molecular bands.[2,3] Single-pulse shock tube experiments of the tetrafluoroethylene oxidation in the range of 1200° to 2000° K show product distributions of COF_2, CO, CF_4, C_2F_6, and small amounts of C_3F_6 and CO_2.[4] In a shock-tube study of the difluoromethylene-oxygen reaction, infrared measurements have directly identified COF_2 as the initial oxidation product of these reactants. Preliminary results show that at temperatures <2200° K, the COF_2 builds up to a steady concentration behind the shock front and that above 2700° K, a nonequilibrium "overshoot" in COF_2 takes place in the reaction mixture.[5]

From a measurement of the thermal decomposition rates of molecules, the rate constants for their formation can be obtained by the principle of detailed balancing, i.e., taking the ratio of the dissociation rate to the equilibrium constant of the reaction. This approach has previously been used, for example, to determine fluorine-fluorocarbon dissociation and recombination rate constants of CF_4 and CF_3.[6] In the present report another part of fluorocarbon chemical kinetics has been investigated and deals with the thermal decomposition of carbonyl fluoride. A shock tube is employed to dissociate COF_2 in dilute mixtures of argon or nitrogen. The rate of COF_2 decomposition is measured by monitoring the COF_2 fundamental band at 5.25μ with a filtered InSb infrared detector. Rate constants for COF_2 initial dissociation are obtained over a pressure range from about 0.2 to 26 atm between 2400° and 3600° K. The pressure and temperature dependences of these rate constants are expressed in terms of the RRK theory for unimolecular reactions. In addition, the complete COF_2 decomposition records are analyzed with a chemical, nonequilibrium shock-tube program to obtain rate constants for the fluorine extraction and recombination reaction of the COF_2 decomposition mechanism.

II. EXPERIMENTAL PROCEDURE

A. SHOCK TUBE

The COF_2 decomposition experiments were conducted behind incident and reflected shock waves in an emission spectroscopy shock tube and behind reflected shock waves in a shock tube coupled to a time-of-flight mass spectrometer.

The optical shock tube was constructed of 1.5-inch I.D. stainless steel tubing and was designed with a 3.5-foot driver section and a 10-foot driven section. The shock tube and associated gas handling system were pumped down to less than 3×10^{-3} torr with a water-cooled oil diffusion pump; they had a leak rate of about 10^{-3} torr per minute. Cold driving with hydrogen of helium against Mylar diaphragms of 2-mil to 5-mil thickness was used to generate shock waves into the test chamber. The shock velocity was measured with a series of platinum heat-transfer gages situated along the driven section. The output of these gages were displayed on a time-mark folded oscilloscope sweep, operated by a Radionics (Model TWN-2A) triangular wave and marker timing generator. Transit times between stations were measured to within ± 1 μsec. The maximum error in the shock velocity was about ± 0.3 percent and introduced an uncertainty of less than $\pm 15^{\circ}$ K in the calculated incident shock temperature or $\pm 40^{\circ}$ K for the reflected shock. Infrared emission from the shocked gas was monitored with a filtered InSb detector (Type 1SC-301) and was viewed through calcium fluoride windows perpendicular to the shock-tube axis.

The mass spectrometer shock-tube apparatus was constructed from 1-inch I.D. Pyrex glass pipe and has a 5-foot driver section and a 15-foot driven section. A Bendix (Model 14-206) time-of-flight mass spectrometer is attached to the shock tube through the "fast reaction chamber." The reflected shock-heated gas was sampled at the shock-tube endwall, which is a flat stainless steel plate having in its center a hyperbolic nozzle with a 2-mil inlet and 10-mil exit (Englehard Industries, Englehard, New Jersey). Mass spectral recordings were taken at 25-μsec intervals just before and after shock arrival. The time-resolved ion peaks were displayed on a Tektronix 535A oscilloscope in combination with a type CA-preamplifier and multiscan generator.[7] For initial shock-tube pressures of 3 to 8 torr, the background pressure in the mass spectrometer before shock arrival ranged between 10^{-6} and 10^{-5} torr. A complete description of the mass spectrometer shock-tube apparatus may be found in an earlier report.[8]

B. REAGENTS

Infrared measurements of COF_2 decomposition were made behind incident argon and nitrogen shocks containing COF_2 in a mole ratio of 2:100 with the inert gas. The same measurements were made behind reflected shocks using 0.25:100 and 0.5:100 COF_2 argon mixtures. Mass spectral data on the COF_2 decomposition reaction were taken with a 5:100 COF_2-argon mixture. The COF_2 gas used in this study was obtained from Peninsular Chemresearch (Gainesville, Florida) and had a stated purity of 95 percent. Infrared analysis of COF_2 completely decomposed in excess argon showed that the commercial gas contained about 4.4 ± 2.4 percent CO_2. The buffer gases were of research grade (argon, 99.999 percent purity and N_2, 99.997 percent purity).

III. INFRARED MEASUREMENTS

The infrared absorption spectra of the COF_2 molecule is found to consist of a number of vibrational-rotational bands between 2μ and 38μ.(9) Recently in this laboratory, spectral band intensities in the 2μ to 6μ region of COF_2 (Figure 1) have been determined by employing a "fast scanning" monochromator to record the infrared spectra of reflected shock heated samples of COF_2 in excess argon.(10) For the purpose of studying the thermal decomposition kinetics of COF_2, the fundamental vibrational band at 5.25μ was monitored with a filtered InSb detector to observe the time rate of change of the COF_2 concentration behind the shock wave. Examples of infrared oscillogram records depicting COF_2 decomposition at several shock temperature conditions are shown in Figure 2. The COF_2 concentrations of the study were typically less than 2×10^{-7} mole/cc for which the infrared emission at 5.25μ was below 8 percent blackbody intensity over the temperature range of the experiments. Under these conditions, the COF_2 gas was considered optically thin and the measured infrared signal was taken to be linearly dependent on concentration. From the infrared emission peak-height at the shock front and the initial concentration of COF_2 behind the shock wave, each oscillogram record was self-calibrating. It was found in the experiments that the CO decomposition product and the trace amount of CO_2 impurity in the COF_2 reaction mixture radiated in the bandpass of the 5.25μ filter. Corrections to the COF_2 infrared records were made by subtracting out the CO (less than 10 percent) and CO_2 (less than 5 percent) spectra. Necessary correction factors were obtained from measurements of the infrared signal generated by known quantities of CO and CO_2 in argon shocks.

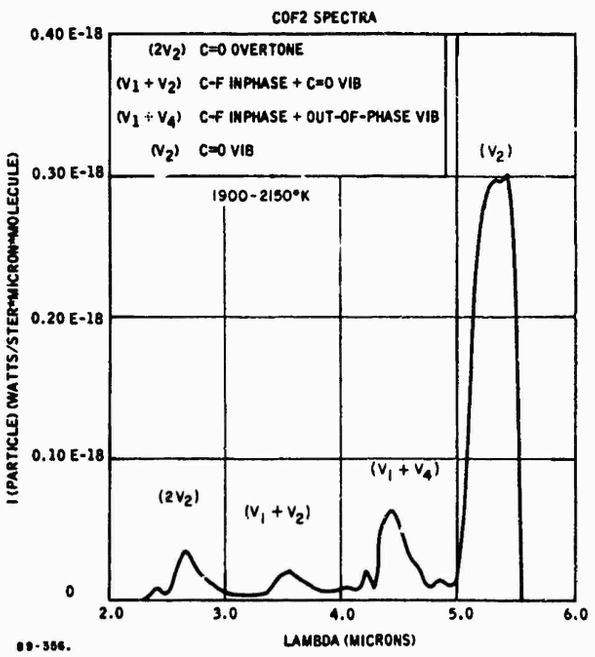

Figure 1 ABOLUTE INTENSITY OF THE COF_2 EMISSION SPECTRA IN THE 2μ TO 6μ REGION

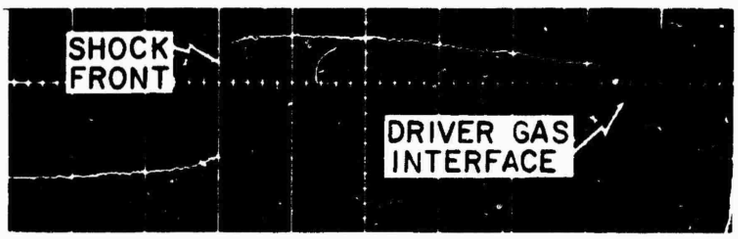

TEMP 2185°K PRESSURE 1.07 atm
50 μ sec BETWEEN VERTICALS

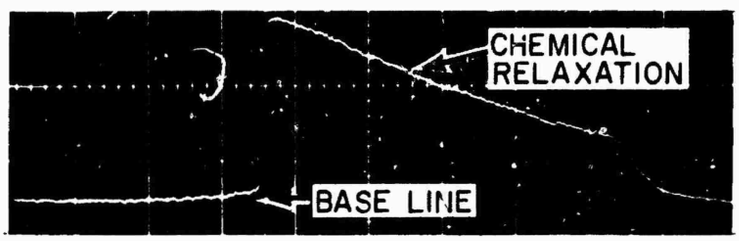

EMISSION ⟶

TEMP 2460°K PRESSURE 1.23 atm
50 μ sec

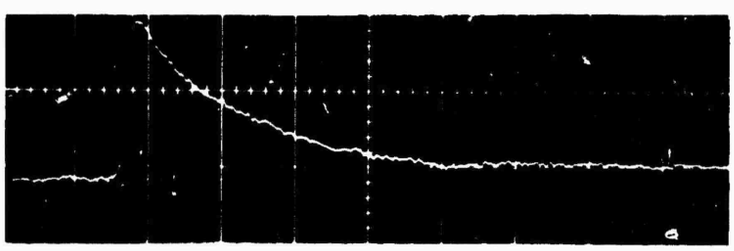

TEMP 3040°K PRESSURE 1.56 atm
20 μ sec

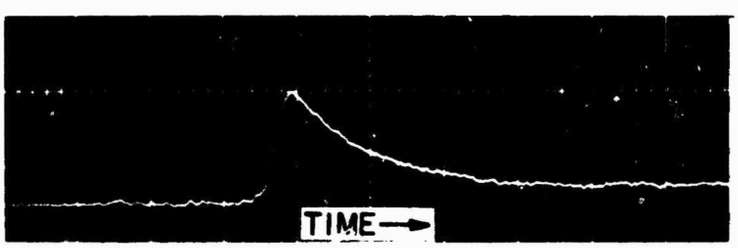

TEMP 3250°K PRESSURE 1.60 atm
10 μ sec

88-7011

Figure 2 EXAMPLES OF COF_2 INFRARED EMISSION AT 5.25μ BEHIND INCIDENT SHOCK WAVES INTO 2:100 COF_2-ARGON MIXTURES

IV. MASS SPECTROMETER MEASUREMENTS

Reaction mixtures of reflected shock-heated COF_2 in excess argon were sampled directly through the shock-tube endwall and analyzed in a time-of-flight mass spectrometer. The mass spectral data were used to study the change in COF_2 mass peak with time (25-μsec intervals after shock compression) and to determine the nature of the decomposition products to gain insight about the COF_2 decomposition mechanism. A typical mass spectra of a COF_2 decomposition mixture is seen in Figure 3. Ion peaks for COF_2(66), COF(47), CO_2(44), Ar(40), Ar(36), and CO(28) are clearly identified. Interestingly, mass peaks for CF_3(69), CF_2(50), and CF(31) are absent in the spectra. The histories of the COF_2 ion peak were used directly to obtain the initial dissociation rate constants for the COF_2 molecule. The mass spectrometer records show that CO is the major molecular end-product of COF_2 decomposition. This observation is in agreement with CO infrared analysis at 4.6μ. It is found that after complete decomposition of COF_2, the CO concentration in the mixtures equals the stoichiometric CO content of the COF_2 molecules present at the beginning of the reaction.

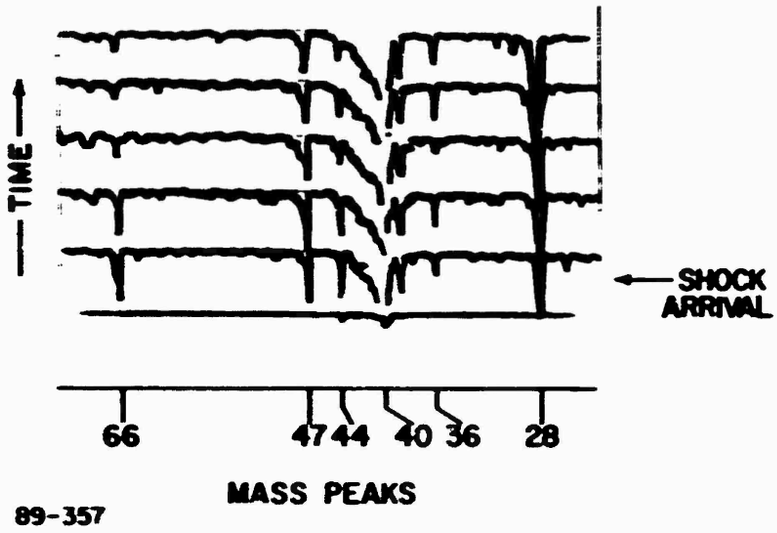

Shock temperature = 3650° K. Pressure = 0.17 atm (5:100 COF_2-argon). Mass analysis = 25 μsec per scan. Mass peaks 66(COF_2), 47(COF), 44(CO_2), 40(Ar), 36(Ar), 28(CO).

Figure 3 MASS SPECTROGRAM OF DECOMPOSED COF_2 BEHIND REFLECTED SHOCK WAVE

V. THERMAL DISSOCIATION RATE CONSTANT OF CARBONYL FLUORIDE

The kinetics of COF_2 thermal dissociation were studied over a pressure range from about 0.2 to 26 atm in argon shocks, and from about 0.4 to 1.5 atm in shock-heated nitrogen. The temperature interval of the data extended from 2400° to 3600° K. The rate constant for thermal dissociation of COF_2

$$\text{R1} \quad COF_2 \xrightarrow{Ar, N_2} COF + F$$

was determined from the initial slope of the infrared emission records, corresponding to the first 10-percent decay in the COF_2 concentration. Some dissociation rate constants were also measured off mass spectrometer oscillogram records for 50 percent COF_2 dissociation. The "apparent" dissociation rate constant defined by

$$\frac{d[COF_2]}{[COF_2]dt} = k_{Obs} \quad (1)$$

where $[COF_2]$ is the COF_2 concentration behind the shock wave, is plotted against reciprocal temperature in Figures 4 and 5. The average total concentration associated with each set of dissociation rate constants is denoted by a normalized density equal to the density of the shocked gas divided by the density of the gas at 1 atm pressure and 273° K. Examples of the shock tube experiments performed in this study are given in Table I.

It is seen from the data of Figures 4 and 5, that the apparent first-order rate constants are neither independent nor linearly dependent on total concentration, but rather show a systematic fall-off with concentration at a given temperature. This type of behavior for thermal dissociation reactions of polyatomic molecules has been explained by a number of theoretical formulations.[11-13] The COF_2 dissociation rate constants of this work are fitted by the general rate constant equation derived from the Rice-Ramsperger-Kassel (RRK) theory on unimolecular reactions. The general rate constant formula of the RRK theory is given by

$$k(RRK) = \frac{A e^{-\frac{E_o}{RT}}}{m!} \int_o^\infty \frac{x^m e^{-x} dx}{1 - (AT^{-0.5} cZ)\left[x / \left(\frac{E_o}{RT} \cdot x\right)\right]^m} \quad (2)$$

where $k_\infty = A e^{-\frac{E_o}{RT}}$ is the Arrhenius high-pressure rate constant. E_o is the minimum energy for dissociation. A is the frequency factor. The quantities m, c, and Z, are the number of effective oscillators participating in the dissociation process, the total concentration, and the effective collision frequency. x is the dimensionless variable, $(E - E_o)/RT$. The RRK rate constant for COF_2 decomposition compared with the general rate constant from Slater's theory.

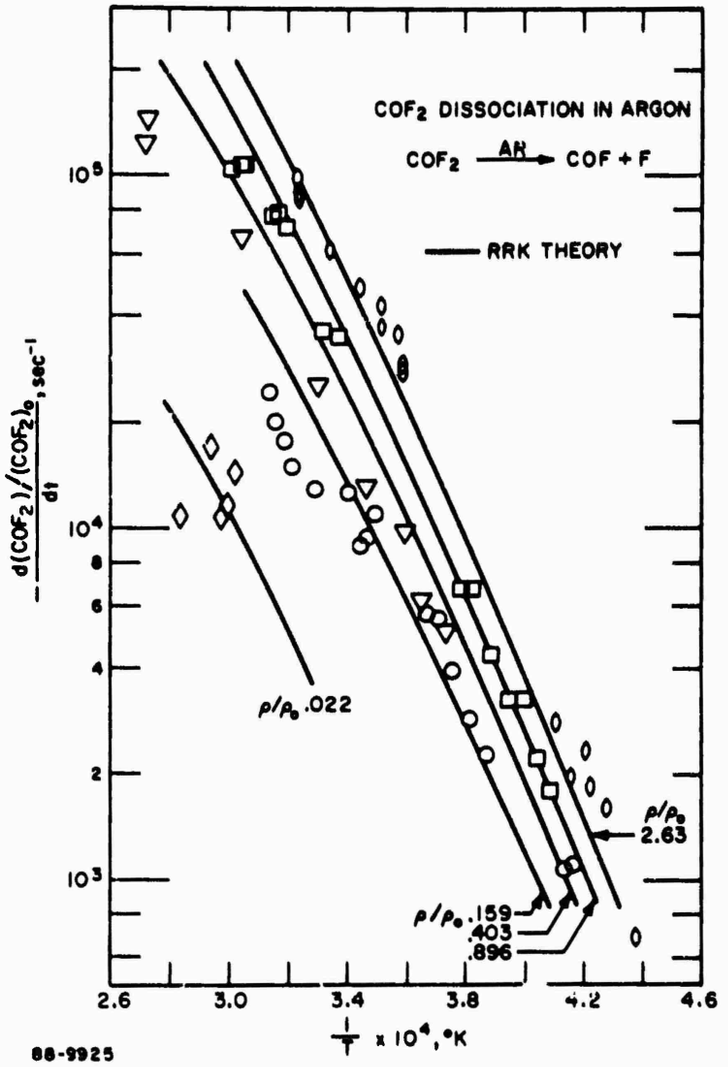

p/p_o is a gas density normalized to density at 1 atm and 273° K. Solid lines are RRK rate integral with $A = 6.14(10^{11})sec^{-1}$, $E_o = 91912$ cal/mole, $m = 6$ and $Z = 7.5(10^{10})$ cc/mole sec. ◇, mass spectrometer data. All other data are from infrared measurements.

Figure 4 APPARENT FIRST-ORDER RATE CONSTANTS OF COF_2 THERMAL DISSOCIATION IN ARGON DILUENT

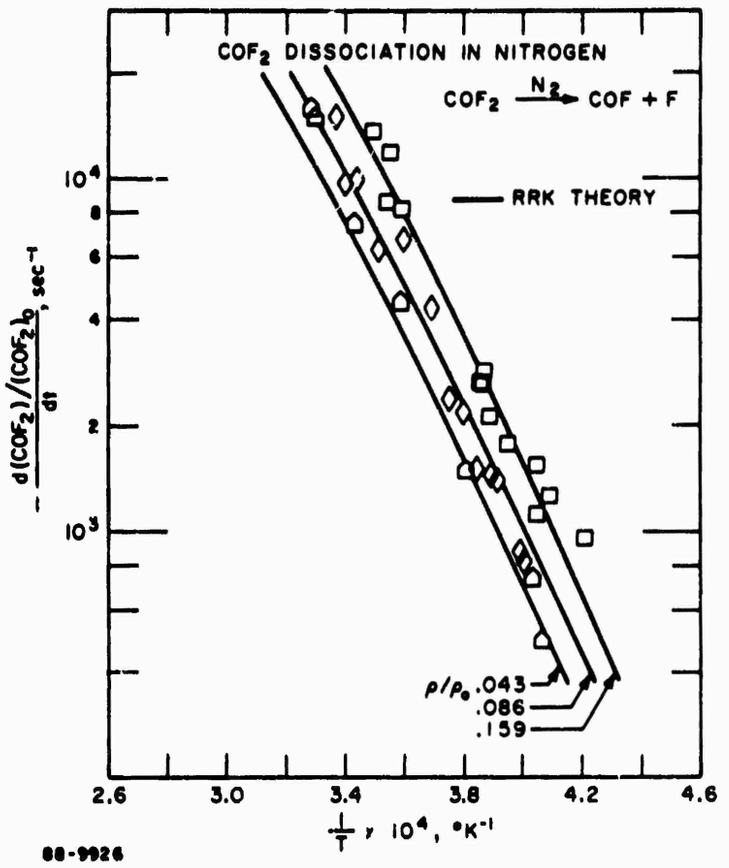

Solid lines are RRK rate integral with $A = 6.14(10^{11})$ sec^{-1}, $E_o = 91912$ cal/mole, $m = 6.0$ and $Z = 1.0(10^{11})$ cc/mole sec.

Figure 5 APPARENT FIRST-ORDER RATE CONSTANTS OF COF_2 THERMAL DISSOCIATION IN NITROGEN DILUENT

TABLE I

COF_2 DISSOCIATION IN ARGON SHOCKS

Experiment No.	Shock Temperature (^oK)	Total Concentration (mole/cc)	Apparent Rate Constant (sec^{-1})	Total Pressure (atm)
2:100 COF_2 - Argon				
1*	2405	6.245×10^{-6}	1.11×10^{3}	1.23
2	2545	6.270×10^{-6}	2.42×10^{3}	1.31
3	2880	6.345×10^{-6}	9.45×10^{3}	1.50
4	3195	6.395×10^{-6}	2.42×10^{4}	1.68
0.5:100 COF_2 - Argon				
5**	2678	1.586×10^{-5}	4.94×10^{3}	3.48
6	2880	2.231×10^{-5}	1.29×10^{4}	5.27
7	3304	1.686×10^{-5}	6.79×10^{4}	4.57
8	3680	1.300×10^{-5}	1.24×10^{5}	3.93
9	2475	3.840×10^{-5}	2.23×10^{3}	7.80
10	2655	3.930×10^{-5}	6.70×10^{3}	8.60
11	3010	4.090×10^{-5}	3.62×10^{4}	10.10
12	3270	4.180×10^{-5}	1.08×10^{5}	11.20
0.25:100 COF_2 - Argon				
13	2343	1.19×10^{-4}	1.62×10^{3}	22.9
14	2410	1.20×10^{-4}	1.93×10^{3}	23.8
15	2795	1.18×10^{-4}	2.71×10^{4}	27.2
16	2905	1.12×10^{-4}	4.91×10^{4}	26.7
17	3100	1.10×10^{-4}	9.88×10^{4}	28.0

*Incident shock data
**Reflected shock data

TABLE I (Concl'd)

COF_2 DISSOCIATION IN NITROGEN SHOCKS

Experiment No.	Shock Temperature (^oK)	Total Concentration (mole/cc)	Apparent Rate Constant (sec^{-1})	Total Pressure (atm)
2:100 COF_2 - Nitrogen				
1*	2460	1.756×10^{-6}	4.88×10^{2}	0.354
2	2615	1.779×10^{-6}	1.45×10^{3}	0.382
3	2795	1.804×10^{-6}	4.42×10^{3}	0.414
4	2915	1.819×10^{-6}	7.39×10^{3}	0.435
5	2555	3.542×10^{-6}	1.38×10^{3}	0.743
6	2715	3.586×10^{-6}	4.27×10^{3}	0.799
7	2840	3.620×10^{-6}	6.23×10^{3}	0.844
8	2970	3.651×10^{-6}	1.50×10^{4}	0.890
9	2478	7.035×10^{-6}	1.53×10^{3}	1.450
10	2590	7.104×10^{-6}	2.61×10^{3}	1.510
11	2796	7.215×10^{-6}	8.15×10^{3}	1.660
12	2863	7.250×10^{-6}	1.34×10^{4}	1.700

*Incident shock-wave data

$$k(\text{Slater}) \quad \frac{A e^{-\frac{E_o}{RT}}}{m!} \int_0^{\infty} \frac{x^m e^{-x}\, dx}{1 + (\theta c)\left[x / \frac{E_o}{RT}\right]^m} \,. \qquad (3)$$

where θ is related to the mean frequency and amplitude factors of vibrational modes leading to reaction. The parameters of Equation (2) giving a best fit to the observed COF_2 rate constant were evaluated as follows. The k_∞'s were determined by plotting the experimentally observed rate constants at a given temperature against pressure (Figure 6) and to a first approximation least squares fitting the data with the phenomenological equation, $k_{obs} = \frac{k_\infty p}{p + r}$, based on the Lindemann mechanism for a unimolecular reaction.[14] The k_∞'s were next used to determine A by a least squares fit of the Arrhenius rate constant, taking E_o = 91.912 kcal/mole* (see Figure 7). The RRK rate integral Equation (2) was solved on an IBM 360 computer for $A = 6.14 \times 10^{11}$ sec^{-1} and E_c = 91.912 kcal/mole where m and Z were varied systematically until a satisfactory fit was achieved with one set of the experimental data (Figure 8). The solid curves in Figures 4 and 5 are the theoretical RRK rate constants and show that with the kinetic parameters

Gas	A sec^{-1}	E_o kcal mole	m	Z cc/mole sec
Argon	$6.14(10^{11})$	91.912	6	$7.5\ 10^{11}$
N_2	$6.14(10^{11})$	91.912	6	$1.0\ 10^{11}$

an accurate correlation (within 40 percent) of both the argon and nitrogen data is obtained over the concentration range of the study. However, it is pointed out here that these values of m and Z are not at all unique in fitting the data. Reasonable curve fits within the scatter of the experimental points are also obtained for m = 4 and $Z = 5.0 \times 10^{11}$ cc/mole sec. Calculations with the RRK integral for m = 6 equally can show agreement with the experimental data.

*In order to be consistent with current JANAF thermochemical data, the first and second bond dissociation energies of COF_2 were based on the enthalpy change for the reaction $CO_2 = CO + 2F$, $\Delta H_r = 160.5$ kcal/mole and were taken to be in the same ratio as the first and second bond dissociation energies of CF_4. Analogous to $D(F - CF_3)/D(F - CF_2) = 1.34$, the values of $D(F - COF)$ and $D(F - CO)$ are 91.912 and 68.57 kcal/mole, respectively.

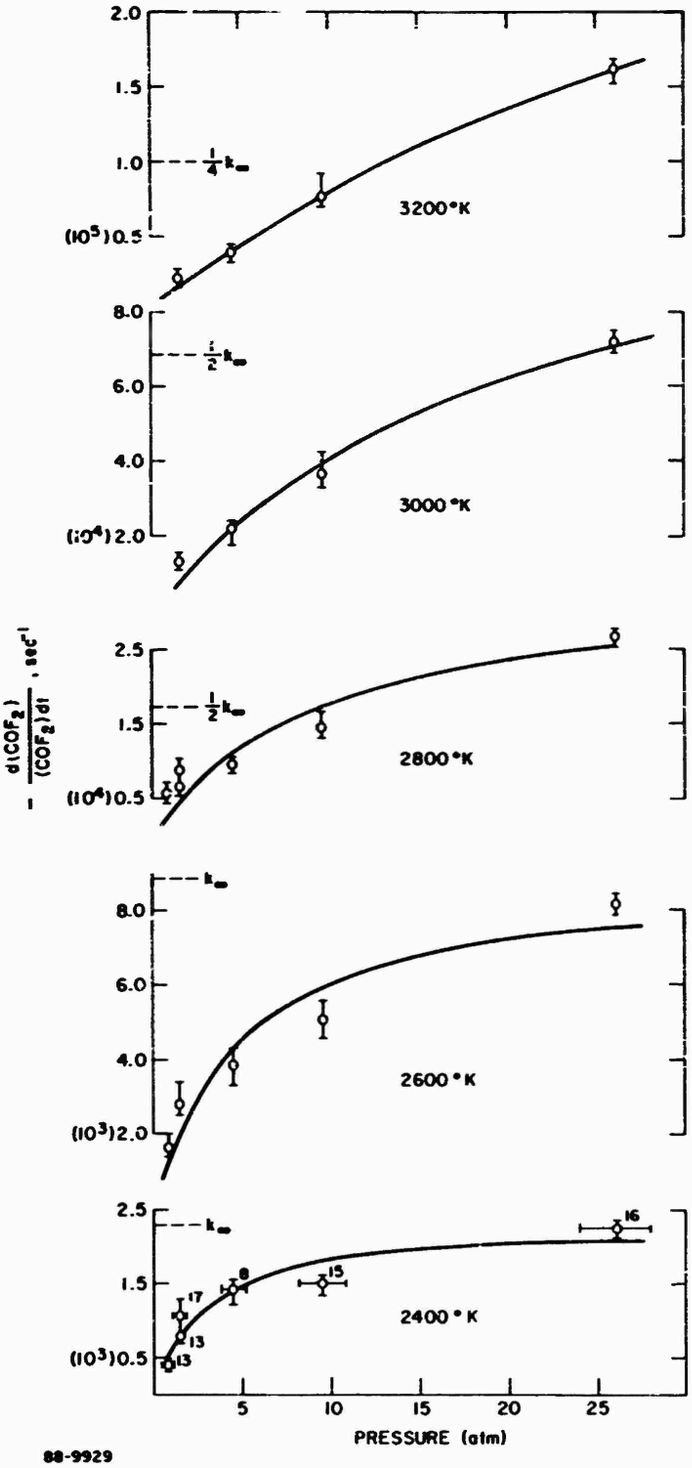

Vertical bar indicates experimental scatter of data. Horizontal bar shows pressure interval of data point. Number of experiments used to evaluate data point near a given pressure appears beside vertical bar. Solid lines are nonlinear least squares fit of data with $k_{obs} = k_\infty p/p + r$.

Figure 6 PRESSURE DEPENDENCE OF COF_2 DISSOCIATION RATE CONSTANT WITH TEMPERATURES

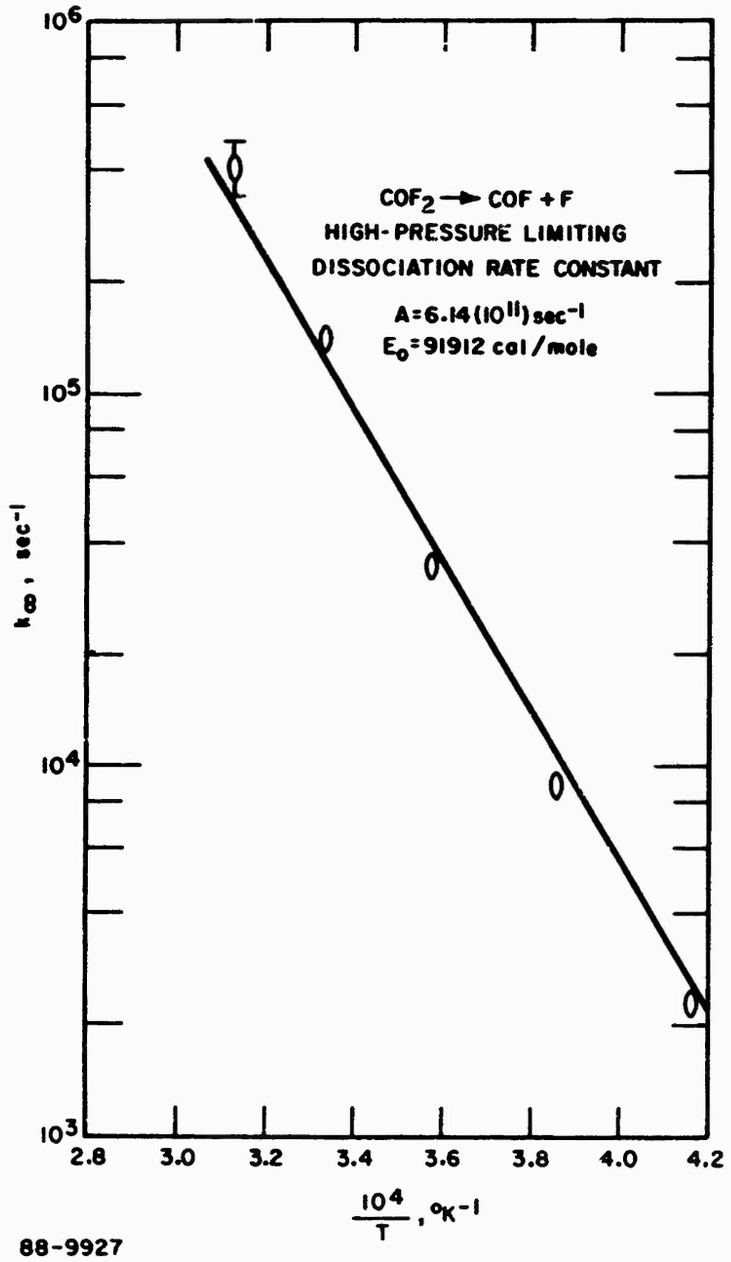

Vertical bar shows statistical spread of k_∞ values.

Figure 7 LEAST SQUARES FIT OF EXTRAPOLATED LIMITING HIGH-PRESSURE RATE CONSTANT WITH ARRHENIUS FORMULA FOR E_0 = 91912 CAL/MOLE

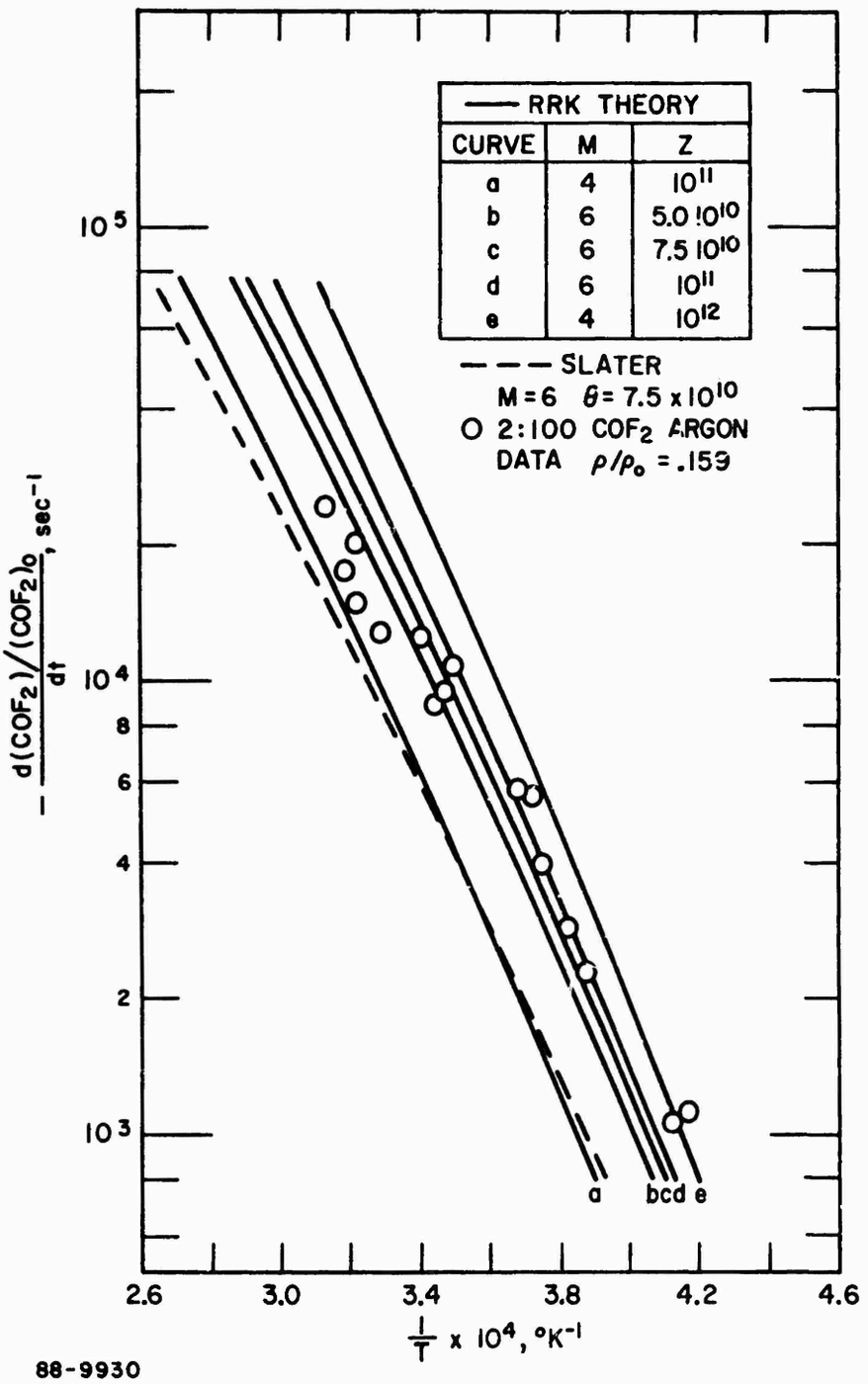

Figure 8 PARAMETRIC ANALYSIS OF COF_2 FIRST-ORDER RATE CONSTANTS WITH RRK AND SLATER RATE INTEGRALS

VI. MECHANISM AND KINETICS OF CARBONYL FLUORIDE DECOMPOSITION

Mass spectrometer and infrared evidence show that under the experimental conditions of this study COF_2 would mainly decompose to CO and fluorine atoms. A set of reactions which would lead to these results are the thermal dissociation reactions of COF_2 and COF, the fluorine extraction reactions, and the COF disproportionation reaction (Table II). The rate constant of R1 was obtained, as described in the preceding section, from the initial decay in the infrared records of COF_2 behind the shock front. The thermal dissociation rate constant of the COF radical (R2) is based on the difference in the first and second bond dissociation energies, D(F-COF) = 91912 cal/mole and D(F-CO) = 68570 cal/mole of the COF_2 molecule. The rate constants for the fluorine extraction reactions and COF disproportionation reaction were derived from an Arrhenius expression by incorporating the energy of reaction at 0^o K in the exponential term and curve fitting measured COF_2 profiles over the complete chemical relaxation period to establish the magnitude of the pre-exponential factor. Calculated COF_2 profiles are obtained from a nonequilibrium shock-tube computer program which solves simultaneously the Rankine-Hugoniot differential equations for a normal shock wave and the appropriate chemical kinetic equations. The present shock-tube computer program also includes the effect of wall boundary layer on the temperature and density behind the shock front (Appendix A). Species profiles typical of a chemically relaxing shock wave into a 2:100 COF_2-Ar mixture are displayed in Figure 9. Also depicted in the figure are the chemical rates of the decomposition reactions. It is seen that for these particular experimental conditions, the COF_2 thermal dissociation rate (R1) dominates the first 20 percent of COF_2 decomposition and then later R5' becomes the most important path for COF_2 removal. The reasonableness with which the chemistry and rate constants in Table II can predict the experimental COF_2 decomposition profiles for a number of experimental shock conditions is demonstrated by the results in Figure 10. The solid curves in the figure are computed with the non-equilibrium shock-tube program including wall boundary layer effects. The broken curve is calculated without the boundary layer corrections to temperature and density behind the shock front. For the experimental conditions chosen, the boundary layer effect is negligible near the shock front, but does have a noticeable influence on the analysis of the data taken at long times behind the shock wave. In Figure 11, various chemical models for COF_2 decomposition are compared to assess their compatibility with the experimental data. According to the sensitivity of the rate data and the results shown in Figure 11, the rate constants of Table II are considered to be the most probable values within a spread of a factor of ten.

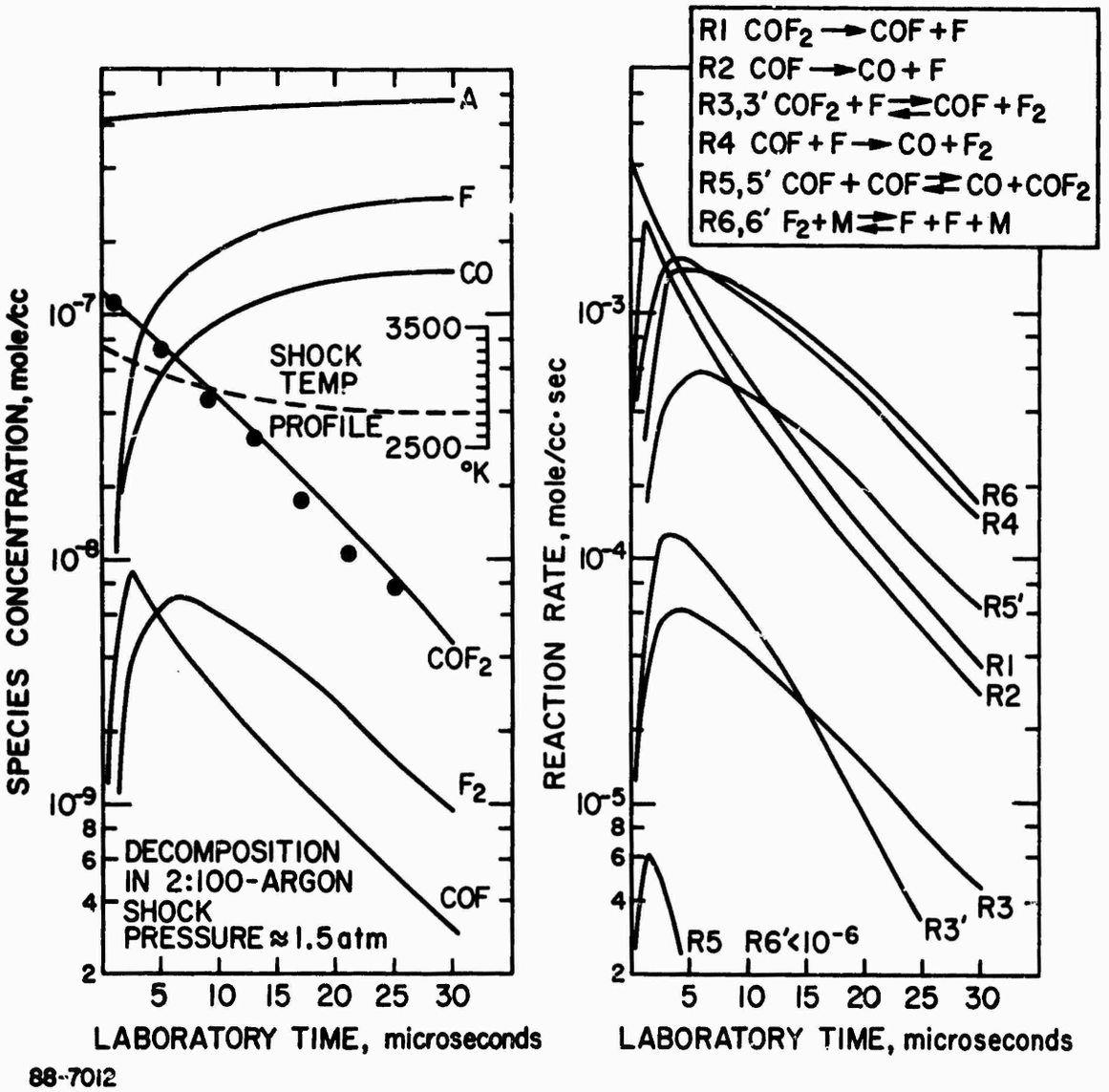

●, experimental COF_2 infrared measurements. Solid lines were calculated with chemistry and rate constants of Table II.

Figure 9 NONEQUILIBRIUM STREAM-TUBE SPECIES PROFILES BEHIND INCIDENT SHOCK WAVE IN A 2:100 COF_2-ARGON MIXTURE

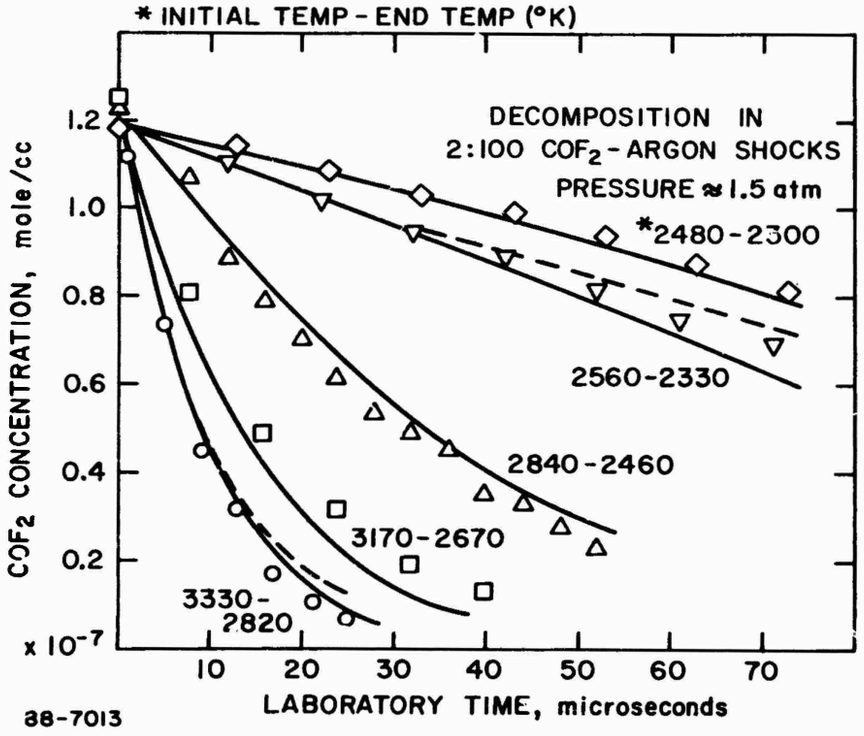

Symbols are experimental infrared data. Solid lines are nonequilibrium stream-tube kinetic profiles including wall boundary layer effects. Broken lines are same calculations with wall boundary-layer effect deleted.

Figure 10 COF_2 HISTORY BEHIND INCIDENT SHOCK WAVES

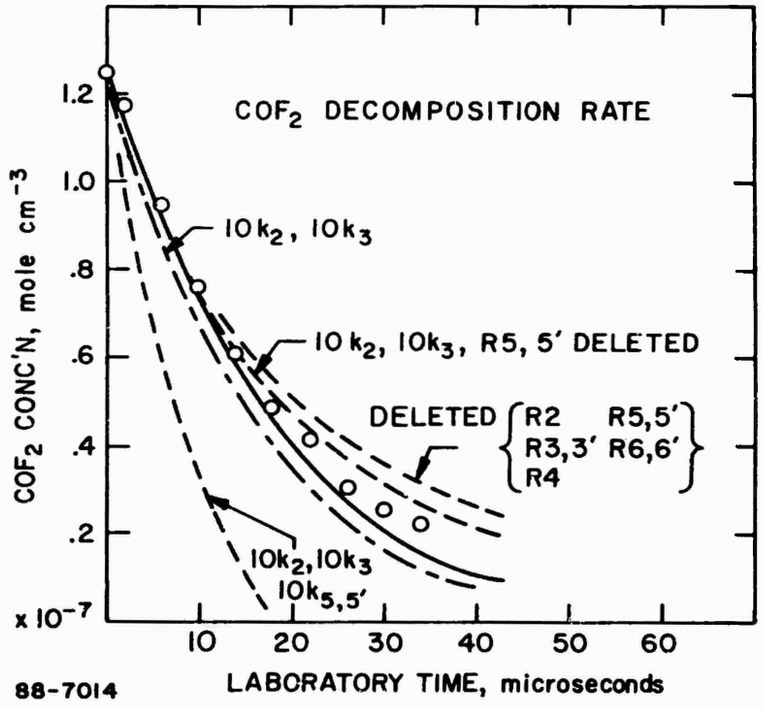

O, experimental infrared data of decomposed 2:100 COF_2-argon mixture at 1.5 atm and 3095° K.

Figure 11 COMPARISON OF SEVERAL CHEMICAL MODELS FOR COF_2 DECOMPOSITION BEHIND INCIDENT SHOCK WAVES

TABLE II

CHEMISTRY AND RATE CONSTANTS FOR COF_2 DECOMPOSITION

Reaction	[a]Rate Constant
R1 $COF_2 \xrightarrow{Ar} COF + F$	[b] $1.07(10^{11})\, e^{-44910/T} \int_0^\infty \frac{\epsilon^s e^{-\epsilon}\, d\epsilon}{1 + \frac{2.09\, 1^{-0.5}}{\epsilon}\left[\frac{\epsilon}{(44910/T) - \epsilon}\right]^5}$
R2 $COF \xrightarrow{Ar} CO + F$	[b] $1.07(10^{11})\, e^{-44910/T} \int_0^\infty \frac{\epsilon^4 e^{-\epsilon}\, d\epsilon}{1 + \frac{2.09\, 1^{-0.5}}{\epsilon}\left[\frac{\epsilon}{(44910/T) - \epsilon}\right]^4}$
R3 $COF_2 + F \rightarrow COF + F_2$	$1.0(10^{13})\, T^{0.5}\, e^{-27740/T}$
R3' $COF + F_2 \rightarrow COF_2 + F$	[c] $4.52(10^{10})\, T^{0.5}\, e^{-1049/T}$
R4 $COF + F \rightarrow CO + F_2$	$1.0(10^{13})\, T^{0.5}\, e^{-1649/T}$
R5 $COF + COF \rightarrow COF_2 + CO$	[c] $1.07(10^{9})\, T^{0.5}\, e^{-605/T}$
R5' $COF_2 + CO \rightarrow COF + COF$	$1.0(10^{11})\, T^{0.5}\, e^{-11656/T}$
R6 $F_2 + Ar \rightarrow F + F + Ar$	[d] $1.52(10^{12})\, e^{-1204/T}$
R6' $F + F + Ar \rightarrow F_2 + Ar$	[d] $1.46(10^{11})\, e^{-6007/T}$

[a] Units of cubic centimeters, °K, mole, and sec. Energy of reaction in exponential terms is calculated from heat-of-formation of 0° K for COF_2 (ΔH_f = -150.96 kcal/mole), COF (ΔH_f = -77.41 kcal/mole), CO (ΔH_f = -27.2 kcal/mole and F (ΔH_f = 18.36 kcal/mole).

[b] RRK rate constant obtained by curve-fitting 2:100 COF_2-Argon kinetic data for total concentration of 6.2 (10^{-6}) mole/cm^3. M is taken to be maximum number of vibrational degree of freedom for a nonlinear COF molecule. Critical frequency is assumed to be same as first (C-F) bond in COF_2.

[c] Pre-exponential factor determined from JANAF entropy-of-reaction and curve-fit of reverse reaction.

[d] Obtained from experimental dissociation rate constant [R. W. Diesen, J. Chem. Phys. 44, 1661 (1961)] and JANAF equilibrium constant.

VII. DISCUSSION

Apparent rate constants for COF_2 dissociation between 2400° to 3600° K exhibited a marked fall-off as the pressure of inert gas was increased over a 100-fold range. The Arrhenius pre-exponential factor A obtained by extrapolating the experimental data to the high-pressure unimolecular limit appears to be in agreement with values (10^{12} to 10^{14} sec^{-1}) usually considered "normal" for unimolecular reactions. The number of "effective" oscillators used in the RRK rate integral to fit the apparent first-order rate constants was chosen to be 6, which is the total number of normal modes in COF_2 and the maximum number permitted by theory for this type of molecule. Values of m less than 6 were not considered because they result in fits whose temperature dependences are qualitatively steeper than the trend indicated by the data. Use of values greater than 6 would have been contradictory to theory. Although the kinetic parameters expressing the experimental dissociation rate constants of this work may be somewhat vagarious, nontheless, it will be interesting to use them as examples to treat other theoretical relations which might want to be compared with experiment.

For hard spheres, the classical collision frequency Z is $\sigma_{12}^2 N \left(\frac{8\pi kT}{\mu}\right)^{1/2}$ which is 9.1×10^{12} cc/mole sec for COF_2-argon partners and 1.1×10^{13} for COF_2-N_2 partners (the collision diameters are taken to be $\sigma_{Ar} = 3.4A$, $\sigma_{N_2} = 3.71A$ and $\sigma COF_2 = 4.6A$, the mean diameter of CO_2 and CF_4).[15] A comparison of the hard-spheres collision frequency with experiment yields steric factors of 0.008 and 0.009 for COF_2 dissociation by argon and nitrogen. The steric factor generally is associated with the fraction of collisions that cause dissociation of critically energized molecules and is considered to be a measure of the steric hindrance in the colliding pair.

Theoretically the transition pressure for a unimolecular reaction is approximately related to the high-pressure frequency factor A by

$$A[\Delta E'(E_o - \Delta E)]^m RT = pZ \qquad (4)$$

where at moderate pressures ΔE on the average has the value $(m + 1)$ RT.[16] With $E_o = 91.912$ kcal/mole and the experimental values of $m = 6$, $A = 6.14 \times 10^{11}$ sec^{-1}, the transition pressure for the unimolecular dissociation of COF_2 in argon at 3000° K is calculated to be 15.4 atm, which appears to be in line with the observed pressure dependence (Figure 6).

The concept that in a unimolecular reaction the activated complex is in quasi-equilibrium with the normal molecule has led to the formulation of Eyring's transition state theory and a rationale for the Arrhenius pre-exponential factor. The quantity A is related

$$A = \left(\frac{kT}{h}\right) \frac{Q^{\ddagger}}{Q} \qquad (5)$$

where Q^1 is the partition of the activated complex and Q is the partition function of the normal molecule. Theoretically to evaluate the pre-exponential factor for the COF_2 unimolecular dissociation, the electronic contribution to the partition function for both the complex and normal molecule is assumed to be unity. The transition-state of the activated COF_2 molecule is next thought of being a CCF fragment bounded by a weakly attached fluorine atom. It is also assumed that the COF fragment rotates and vibrates independently of its satellite fluorine atom. On the basis of the model presented, the rotational partition function of the activated complex was calculated with the moments of inertia for a COF radical. The ratio of the rotational partition function of the activated complex to that of the normal molecule was thus calculated to be 0.348. Moments of inertia for COF_2 and COF were obtained from JANAF thermochemical tables[17]. In its activated state, the deformation modes of the COF_2 molecule are assumed to be drastically weakened in which case the vibration partition function of the complex is largely determined by the ν_1, ν_2, ν_4 modes of the COF_2 molecule, that is, the in-phase (C-F), the (C=O) vibration and the out-of-phase (C-F) vibration. Accordingly, the ratio of the vibrational partition functions was calculated to be 0.316. Substitution of these numbers for the ratio of the partition functions in Equation (5) gives a calculated pre-exponential factor of 6.86×10^{11} sec^{-1} at 3000° K. Although the result is in remarkable agreement with the experimental value, the coincidence is believed to be more fortuitous than real, since the nature of the complex, though reasonably assumed, must be regarded as only a guess.

It is concluded from mass spectra obtained in the present study that the fluorocarbon products CF_4, CF_3, and CF_2, which are produced by C_2F_4 oxidation, do not appear to form by COF_2 decomposition. Infrared measurements of 4.3μ radiation also did not show kinetic evidence for CO_2 production, nor did ultraviolet measurements at 2660 A indicate the existence of CF_2 species in the COF_2 decomposition mixtures. In accordance with these observations, the reactions

$$COF_2 + COF_2 \longrightarrow CO_2 + CF_4$$

$$COF_2 + COF \longrightarrow CO_2 + CF_3$$

$$COF + COF \longrightarrow CO_2 + CF_2$$

$$COF_2 + M \longrightarrow CF_2 + O + M$$

would not appear to be important in the chemistry for COF_2 decomposition.

APPENDIX A

FORMULATION OF A GENERALIZED CHEMICAL NONEQUILIBRIUM STREAM TUBE COMPUTER PROGRAM WITH WALL BOUNDARY LAYER EFFECTS

Recently, Teare[18] has pointed out that in shock-tube chemical kinetic studies, the accuracy of the results may be significantly impaired, if variations in the flow velocity and state properties due to wall boundary layer growth are neglected in the data analysis.[18] Generally it is understood that the presence of wall boundary layer in the shock tube causes the gas behind the shock wave to behave as if it were passing through a divergent channel where the flow velocity decreases and the gas density and thermodynamic temperature increases with increasing distance. An analytical basis for these effects is provided by the theoretical work of Mirels, who has made use of Duff's concept of a "limiting separation distance" to obtain a local similarity solution for the boundary layer displacement thickness.[19] The constraints placed on the problem require that the mass per unit time integrated over the entire shock tube area be conserved and that the mass of gas entering the shock front be equal to the mass entering the boundary layer at the limiting separation distance.

For the purpose of analyzing shock-tube chemical kinetic data taken at long times behind the shock front, a nonequilibrium stream-tube computer program has been developed to include area variation due to wall boundary layer growth. The quantities describing the flow in wave-stationary coordinates are shown in Figure A-1 which is similar to the diagram given in Reference 19. The "jump" conditions across the shock wave are obtained from the Hugoniot conservation equations,

mass: $\rho_1 U_s = \rho_{eo} u_{eo}$

momentum: $P_1 + \rho_1 U_s^2 = P_{eo} + \rho_{eo} u_{eo}^2$

enthalpy: $h_1 + \frac{1}{2} U_s^2 = h_{eo} + \frac{1}{2} u_{eo}^2$

The equations governing the chemical relaxation zone behind the shock wave are expressed in time differential form by

continuity: $$\frac{d(\rho u A)}{d\zeta_p} \Bigg|_{\rho_1 U_s A_0}^{\rho_e u_e A} = 0$$

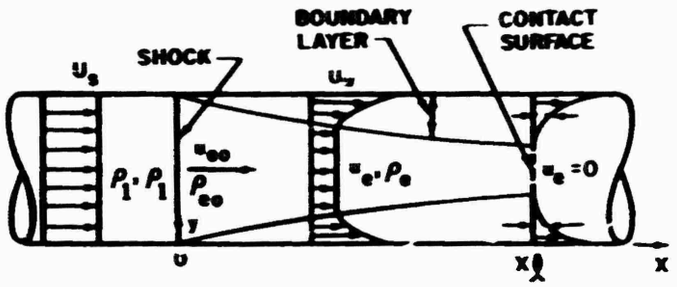

SYMBOLS:

A SUBSONIC FLOW CROSS-SECTIONAL AREA, PRE-EXPONENTIAL FACTOR

c SPECIES CONCENTRATION

E ACTIVATION ENERGY

h STATIC ENTHALPY

M GRAM MOLECULAR WEIGHT

n TEMPERATURE EXPONENT

p STATIC PRESSURE

R IDEAL-GAS CONSTANT

T THERMODYNAMIC TEMPERATURE

t TIME

U SUBSONIC FLOW VELOCITY

U_s SHOCK WAVE VELOCITY

x DISTANCE BEHIND SHOCK WAVE

x_f LIMITING SEPARATION DISTANCE

ρ DENSITY

ν REACTANT STOICHIOMETRIC-COEFFICIENT

SUBSCRIPTS:

1 CONDITION AHEAD OF SHOCK WAVE

0 SHOCK FRONT CONDITION

e CONDITION BEHIND SHOCK WAVE

f FORWARD REACTION

i,k PROPERTY OF i'TH SPECIES, ETC.

i i'TH REACTION

l LABORATORY COORDINATE

P PARTICLE COORDINATE

r REVERSE REACTION

Figure A-1 SHOCK TUBE FLOW DIAGRAM FOR FIXED SHOCK WAVE COORDINATE SYSTEM INCLUDING WALL BOUNDARY LAYER DEVELOPMENT

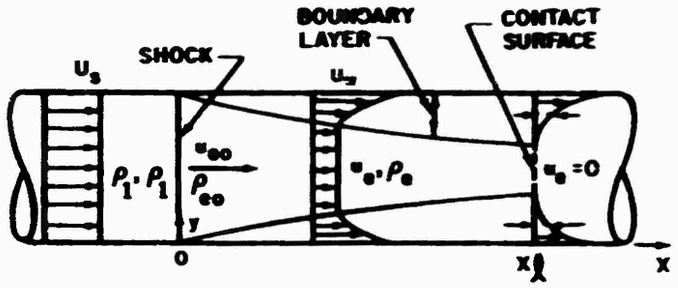

SYMBOLS:

A SUBSONIC FLOW CROSS-SECTIONAL AREA, PRE-EXPONENTIAL FACTOR

c SPECIES CONCENTRATION

E ACTIVATION ENERGY

h STATIC ENTHALPY

M GRAM MOLECULAR WEIGHT

n TEMPERATURE EXPONENT

p STATIC PRESSURE

R IDEAL-GAS CONSTANT

T THERMODYNAMIC TEMPERATURE

t TIME

U SUBSONIC FLOW VELOCITY

U_s SHOCK WAVE VELOCITY

x DISTANCE BEHIND SHOCK WAVE

x_f LIMITING SEPARATION DISTANCE

ρ DENSITY

ν' REACTANT STOICHIOMETRIC-COEFFICIENT

SUBSCRIPTS:

1 CONDITION AHEAD OF SHOCK WAVE

0 SHOCK FRONT CONDITION

e CONDITION BEHIND SHOCK WAVE

f FORWARD REACTION

i,k PROPERTY OF i'TH SPECIES, ETC.

i i'TH REACTION

ℓ LABORATORY COORDINATE

P PARTICLE COORDINATE

r REVERSE REACTION

Figure A-1 SHOCK TUBE FLOW DIAGRAM FOR FIXED SHOCK WAVE COORDINATE SYSTEM INCLUDING WALL BOUNDARY LAYER DEVELOPMENT

momentum: $$\frac{dp}{dt_p} + u \frac{du}{dt_p} \Bigg|_{\tau_1 \rho_1 U_s}^{p_e \rho_e u_e} = 0$$

enthalpy: $$\frac{d(h + 1/2\, u^2)}{dt_p} \Bigg|_{h_1 U_s}^{h_e u_e} = 0$$

For a laminar boundary layer (Reynolds number less than 5×10^7) the area variation of the divergent channel from Mirels' results is given by

$$A_0/A = 1 - (x/x_f)^{0.5}$$

The ideal-gas equation,

$$p = \left(\rho \sum c_i \Big/ \sum c_i M_i\right) RT ,$$

is used to relate the thermodynamic temperature to pressure and density. The molar enthalpy of each species is expressed in terms of temperature by a power series,

$$h_i = \left[L_1 T + \frac{1}{2} L_2 T^2 + \frac{1}{3} L_3 T^3 + \frac{1}{4} L_4 T^4 - L_5 T^{-1} + L_6\right]_i ,$$

in which the temperature coefficients are determined from curve fits of JANAF thermochemical data. The variation in species concentration resulting from chemical reaction and volumetric change behind the shock wave is given by

$$\frac{dc_i}{dt_p} - \frac{c}{\rho} \frac{d\rho}{dt_p} = \sum \pi \nu_{ki}\, c_k\, A_{fj}\, T^{n_j} \exp \frac{E_{fj}}{RT}$$

$$- \sum \pi \nu_{ij}\, c_i\, A_{rj}\, T^{n_j} \exp \frac{E_{rj}}{RT} ,$$

where the positive term on the right of the equality reflects the sum of the chemical rates leading to species production and the negative term, the rates for removal. Events measured in laboratory time are related to the particle time in the shock tube by

$$t_f = \frac{x}{U_s} = \int \left(\frac{u_e}{U_s}\right) d t_p \ .$$

The above set of differential equations is solved on an IBM 360 computer, using a fourth-order predictor-corrector integration scheme. The predictor-corrector method was devised to vary its own integration interval depending on the estimated truncation error available at each step. A Runge-Kutta method was used to obtain the starting values.[20] However, a computational difficulty imposes itself on the formulation of this type of problem, since the time derivative of the area goes to infinity when x approaches zero. Teare[18] has overcome this singularity by assuming for small x's that the area variation is a linear function dependent on the translational/rotational relaxation thickness of the shock wave. In the present program, the computational difficulty is avoided by simply introducing an arbitrary parameter to start the area change at an infinitesimal distance behind the shock front. Calculations show that the results are virtually unaffected by this parameter for values less than 0.0001 of the chemical relaxation distance.

The computer program is general in that the inputs to the calculation are the shock velocity, the state of the gas ahead of the shock wave, and the chemical species and reactions to be considered. The thermodynamic properties of the species used in the calculation are automatically furnished by a computer-tape library containing information on almost every molecule which may be of interest for shock tube study. The computer program is capable of solving chemistry problems with up to 100 reactions and 200 species.

REFERENCES

1. Kupel, R. E., et al., Mass Spectrometric Identification of Decomposition Product of Polytetrafluorethylene and Polyfluorethyleneproylene, Analytical Chemistry 36, 386 (1964).

2. Wentink, T. and W. Planet, Infrared Transmittance and Emittance of Polytetrafluoroethylene, J. Opt. Soc. Am. 51, 601 (1961).

3. Greenberg, R. A., N. H. Kemp and K. L. Wray, Structure of the Laminar Ablating Air-Teflon Boundary Layer, Avco Everett Research Report 301 (1968).

4. Bauer, S. H., K. C. Hou and E. L. Resler, Jr., Single-Pulse Shock Tube Studies of the Pyrolysis of Fluorocarbons and of the Oxidation of Perfluoroethylene, Proceedings: 6th International Shock Tube Symposium, Freiburg, Germany (April 1967) p. 504.

5. Modica, A. P., A Kinetic Model for Teflon-Air High Temperature Chemistry, Avco Report AVSSD-046-67-RR (1968).

6. Modica, A. P., and S. J. Sillers, Experimental and Theoretical Kinetics of High-Temperature Fluorocarbon Chemistry, J. Chem. Phys. 48, 3283 (1968).

7. Glass, G. P., et al., Mechanism of the Acetylene-Oxygen Reaction in Shock Waves, J. Chem. Phys. 42, 608 (1965).

8. Modica, A. P., Kinetics of the Nitrous Oxide Decomposition by Mass Spectrometry: A Study to Evaluate Gas Sampling Methods Behind Reflected Shock Waves, J. Phys. Chem. 69, 2111 (1965).

9. Nielson, A. H., et al., The Infrared and Raman Spectra of F_2CO, FClCO and Cl_2CO, J. Chem. Phys. 20, 596 (1952).

10. Modica, A. P., and R. R. Brochu, COF_2 Band Intensities in the 2.0 ~6.0 Micron Region, Avco Report AVSSD-0130-68-CR (1968).

11. Slater, N. B., Theory of Unimolecular Reactions (Ithaca, New York, Cornell University Press, 1959).

12. Bunker, D. L., Theory of Elementary Gas Reaction Rates (New York, Pergamon Press, 1966).

13. Keck, J., and A. Kalelkar, Statistical Theory of Dissociation and Recombination for Moderately Complex Molecules, Avco Everett Research Report 289 (1968).

14. Benson, S. W., The Foundation of Chemical Kinetics, (New York, McGraw-Hill Book Co., Inc., 1960), pp. 223, 224.

15. Hirshfelder, J. O., C. F. Curtiss and R. B. Bird, Molecular Theory of Gases and Liquids (New York, John Wiley and Sons, Inc., 1954) p. 111.

REFERENCES (Concl'd)

16. Benson, S. W., Ref. 14, pp. 230, 231.

17. JANAF Thermochemical Tables, ed.: D. R. Stull, (Midland, Michigan, Dow Chemical Co.).

18. Camac, M., R. M. Feinberg and J. D. Teare, The Production of Nitric Oxide in Shock-Heated Air, Avco Everett Research Report 245 (1966).

19. Mirels, H., Test Time in Low Pressure Shock Tubes, Phys. Fluids 6, 1201 (1963).

20. Ralston, A., and H. S. Wilf, Mathematical Methods for Digital Computers (New York, John Wiley and Sons, Inc., 1964).

Unclassified

Security Classification

DOCUMENT CONTROL DATA - R & D

(Security classification of title, body of abstract and indexing annotation must be entered when the overall report is classified)

1. ORIGINATING ACTIVITY (Corporate author) Avco Government Products Group Space Systems Division Lowell Industrial Park, Lowell, Massachusetts 01851	2a. REPORT SECURITY CLASSIFICATION Unclassified 2b. GROUP

3. REPORT TITLE

Chemical Kinetics of COF_2 Decomposition in Shock Waves

4. DESCRIPTIVE NOTES (Type of report and inclusive dates)

Technical Report

5. AUTHOR(S) (First name, middle initial, last name)

A. P. Modica

6. REPORT DATE 15 November 1968	7a. TOTAL NO. OF PAGES 38	7b. NO. OF REFS 20
8a. CONTRACT OR GRANT NO. F04-701-68-C-0036 b. PROJECT NO. c. d.	9a. ORIGINATOR'S REPORT NUMBER(S) AVSSD-0247-68-RR 9b. OTHER REPORT NO(S) (Any other numbers that may be assigned this report) SAMSO-TR-69-145	

10. DISTRIBUTION STATEMENT

This document has been approved for public release and sale; its distribution is unlimited.

11. SUPPLEMENTARY NOTES None	12. SPONSORING MILITARY ACTIVITY Space and Missile Systems Organization Deputy for Reentry Systems Air Force Systems Command Norton Air Force Base, California 92409

13. ABSTRACT

An infrared technique has been used to monitor the thermal decomposition of carbonyl fluoride (COF_2) in argon and nitrogen diluent behind incident and reflected shock waves. Data was taken in the temperature range 2400° to 3600° K at total pressures between 0.2 and 26 atm. Direct sampling of reflected shock mixtures with a time-of-flight mass spectrometer provided knowledge of the decomposition products. The pressure and temperature dependence of the COF_2 dissociation rate constants are discussed in terms of the Rice-Ramsperger-Kassel (RRK) unimolecular theory. Rate constants for the fluorine extraction reactions and COF disproportionation reaction were obtained by curve-fitting the complete COF_2 kinetic histories with computed profiles. A chemical nonequilibrium stream-tube program which includes wall boundary layer effects was used for data analysis.

DD FORM 1 NOV 68 1473

Unclassified

Security Classification

14. KEY WORDS	LINK A		LINK B		LINK C	
	ROLE	WT	ROLE	WT	ROLE	WT
Teflon Oxidation						
Infrared Spectra						
Carbonyl Fluoride						
Temperature Dependence						
Shock Waves						
Chemical Kinetics						
Stream-Tube Program						